RECENT RESULTS ON HIGHER ORDER QCD CORRECTIONS TO HADRONIC CROSS SECTIONS*

W.L. van Neerven

Instituut-Lorentz
Univesity of Leiden
P.O. Box 9506, 2300 RA Leiden
The Netherlands

(Received September 19, 1990)

In this lecture recent results obtained from radiative corrections to the Drell–Yan process and heavy flavour production are presented. The K-factors in both processes are large and in the case of heavy flavour production depend very heavily on the choice of the renormalization and factorization scale. The contribution of the gluon-gluon subprocess to both reactions will be discussed.

PACS numbers: 12.38.Bx

Introduction

In the past decade many calculations have been performed on higher order QCD correctios to inclusive and semi-inclusive processes [1]. At present it seems that most of the order α_s corrections to $n \to m$ parton reactions with $n + m \leq 4$ have been computed.

Higher order corrections are necessary for practical as well as theoretical reasons. The practical reason is that the statistics in the ongoing and future experiments will improve, so that higher order corrections will be noticeable. This is expected, as the size of the various K-factors can become rather big. An example is the Drell–Yan (DY) K-factor [2-4] which has been measured in fixed target as well as in proton-antiproton collider experiments. Furthermore it will be interesting to see how these K-factors will behave at very large energies, which are characteristic of future accelarators like LHC and SSC. Here we expect that processes with gluons in the initial state

* Presented at the XXX Cracow School of Theoretical Physics, Zakopane, Poland, June 2–12, 1990

will play a very important role. From the theoretical point of view higher order corrections are interesting because we can learn something about the behaviour of the perturbation series. In particular one wants to understand the various mechanisms which dominate the K-factor. An example is soft gluon radiation which in some regions of phase space constitute the bulk of the radiative corrections. Finally we expect that cross sections,corrected to higher orders in the running coupling constant α_s, are less sensitive to variations in the factorization and renormalization scales than the lowest order ones.

In this lecture I would like to present the results obtained from recent calculations of QCD corrections to the following two processes *i.e.* inclusive vector boson production [5] (DY) and heavy flavour production [6]. In the first case we have calculated a part of the $O(\alpha_s^2)$ corrections to the DY K-factor whereas in the second one we finished the complete $O(\alpha_s)$ correction to the semi inclusive cross section for heavy (anti) quark production. Notice that the latter process has been also calculated by an other group [7] and to a large extent we agree with their results.

In this lecture we apply the methods of perturbative QCD [8] to so-called "hard cross sections". They are denoted by $d\sigma(s_1, s_2 \ldots s_n)$ where s_i are the invariants involved which get asymptotic (*i.e.* $s_i \to \infty$) with s_i/s_j = fixed. Notice that s_i/s_j will neither become zero nor infinite. If one integrates over a subset $\{s_i\}$ then collinear (mass) singularities will show up in the initial or final state. These singularities are removed from the cross section *via* splitting functions which in their turn renormalize the input parton distribution and final state fragmentation functions. In this way these functions become scale dependent. Perturbative QCD is based on the parton model. The succes of this model is the main justification to compute higher order radiative corrections in QCD.

1. Drell–Yan process

Massive vector boson productions is an important process to study the properties of the electroweak bosons W and Z. Moreover it is an important background process in large hadron colliders LHC or SSC in the search for the Higgs or supersymmetric particles. Massive vector boson production or dilepton pair production is given by the reaction

$$\mathrm{H}_1 + \mathrm{H}_2 \to \mathrm{V} + \mathrm{X} \to \ell_1 + \ell_2, \tag{1.1}$$

where V is one of the vector bosons of the standard model (W, Z or γ) which subsequently decays into a lepton pair (ℓ_1, ℓ_2). The symbol X denotes any final hadronic state which momenta are completely integrated over. The colour averaged cross section is given by

$$\frac{d\sigma}{dQ^2} = \tau\sigma_V(Q^2, M_V^2)\, W(\tau, Q^2), \quad \tau = Q^2/S\,, \tag{1.2}$$

where σ_V indicates the pointlike DY cross section. Further S represents the C.M. energy of the incoming hadrons H_1, H_2 and Q^2 stands for the dilepton pair mass. From the DY mechanism it follows that the hadronic structure function $W(\tau, Q^2)$ can be written as

$$W(\tau, Q^2) = \sum_{i,j} \int_0^1 dx_1 \int_0^1 dx_2 \int_0^1 dx\, \delta(\tau - x_1 x_2 x) f_i^{H_1}(x_1, \mu^2) f_j^{H_2}(x_2, \mu^2) \times \Delta_{ij}(x, Q^2, \mu^2, M^2), \tag{1.3}$$

where $f_i^{H_k}$ denotes the parton (gluon, quark) distribution function of hadron H_k which depends on the mass factorization scale μ^2. The QCD correction term denoted by Δ_{ij} depends in addition to the mass factorization scale μ^2 also on the renormalization scale M^2. The DY correction term Δ_{ij} can be inferred from the DY parton structure function $\widehat{W}$ *via* mass factorization

$$\widehat{W}_{ij}(z, Q^2, M^2, \varepsilon) = \sum_{k,l} \int_0^1 dx_1 \int_0^1 dx_2 \int_0^1 dx\, \delta(z - x_1 x_2 x) \Gamma_{ki}(x_1, \mu^2, \varepsilon) \times \Gamma_{lj}(x_2, \mu^2, \varepsilon) \Delta_{kl}(x, Q^2, \mu^2, M^2), \tag{1.4}$$

where $\widehat{W}_{ij}$ corresponds to the parton subprocess

$$i + j \to \mathrm{V} + \mathrm{X}\,, \tag{1.5}$$

and Γ represents the splitting function. Like $\widehat{W}$ it depends on the renormalized coupling constant $\alpha_s(M)$ which has been determined in the $\overline{\mathrm{MS}}$ scheme. The collinear divergences showing up in $\widehat{W}$ and Γ have been regularized by n-dimensional regularization ($\varepsilon \equiv n - 4$). The splitting functions as well as the correction term are mass factorization dependent. In the current literature two schemes have become popular *i.e.* the $\overline{\mathrm{MS}}$ and the DIS scheme. In the first case Γ takes the following form

$$\Gamma_{ij}(x) = \delta_{ij} + \left(\frac{\alpha_s}{4\pi}\right) \frac{1}{\varepsilon} P_{ij}^{(0)}(x) + \left(\frac{\alpha_s}{4\pi}\right)^2 \left[\frac{1}{\varepsilon^2}\left(\tfrac{1}{2} P_{ik}^{(0)} \otimes P_{kj}^{(0)}(x) + \beta_0 P_{ij}^{(0)}(x)\right) + \frac{1}{2\varepsilon} P_{ij}^{(1)}(x)\right]. \tag{1.6}$$

Here $\otimes$ denotes the convolution symbol and the $P_{ij}^{(n)}$ stand for the Altarelli–Parisi splitting functions [8] which are calculated up to $n = 1$. The lowest order coefficient appearing in the series expansion for the beta function is represented by β_0. In the DIS scheme the splitting functions become

$$\Gamma_{qq}(x) = \hat{\mathcal{F}}_{2q}(x, Q^2, M^2, \varepsilon), \; \Gamma_{qg}(x) = \hat{\mathcal{F}}_{2g}(x, Q^2, M^2, \varepsilon), \tag{1.7}$$

where $\hat{\mathcal{F}}_{2q}, \hat{\mathcal{F}}_{2g}$ denote the deep inelastic lepton–hadron parton distribution functions corresponding to the parton subprocesses with a quark or a gluon in the initial state respectively. The disadvantage of this scheme is that Γ_{gq} and Γ_{gg}, can be arbitrarily chosen. However the second moment can be determined in such a way by requiring that the momentum sum rule will be satisfied. In this lecture all our results have been calculated in the DIS scheme. Up to order α_s^2 the DY structure function $\widehat{W}$ Eq. (1.4) receives contributions from the following parton subprocesses

$O(\alpha_s^0)$	$q + \bar{q} \to V$		(1.8)
$O(\alpha_s)$	$q + \bar{q} \to V$	(1 loop)	(1.9a)
	$q + \bar{q} \to V + g$		(1.9b)
	$g + q(\bar{q}) \to V + q(\bar{q})$		(1.10)
$O(\alpha_s^2)$	$q + \bar{q} \to V$	(2 loop)	(1.11a)
	$q + \bar{q} \to V + g$	(1 loop)	(1.11b)
	$q + \bar{q} \to V + g + g$		(1.11c)
	$q + \bar{q} \to V + q + \bar{q}$	(NS+S)	(1.12)
	$g + g(\bar{q}) \to V + q(\bar{q})$	(1 loop)	(1.13a)
	$g + q(\bar{q}) \to V + q(\bar{q}) + g$		(1.13b)
	$q(\bar{q}) + q(\bar{q}) \to V + q(\bar{q}) + q(\bar{q})$	(NI+I)	(1.14)
	$g + g \to V + q + \bar{q}$		(1.15)

The symbols NS (S) in Eq. (1.12) denote the nonsinglet (singlet) part respectively. They refer to the splitting functions needed to render $\widehat{W}$ finite. In Eq. (1.14) we have computed the cross sections for identical (I) as well as nonidentical quarks (NI) in the final state. Till this moment we have not computed the hard gluon contribution in Eq. (1.11c) and the qg subprocess in Eqs. (1.13a) and (1.13b). Since the DY correction term has been calculated in the DIS scheme we need the parton distribution functions in the same scheme in order to determine the hadronic structure function in Eq. (1.3). For that purpose we have chosen the DFLM set 4 [9]. For the running coupling constants we adopt the expression in Eq. (10) of Ref. [10]

which is corrected up to two loops with heavy flavour thresholds included ($\Lambda = 0.2$ GeV). Unless stated otherwise the mass factorization scale μ is chosen to be equal to the renormalization scale M.

In what follows below we will only show results for the total inclusive cross section

$$\sigma_{\rm tot}(S) = \int dQ^2 {\rm BW}(Q^2, M_V{}^2) W(\tau, Q^2), \tag{1.16}$$

where $\mathrm{BW}(Q^2, M_V{}^2)$ denotes the Breit-Wigner form. In the discussion of the results we will try to answer the following questions.

a. How large is the $O(\alpha_s{}^2)$ contribution to the K-factor compared with the $O(\alpha_s)$ one?
b. What is the relative contribution of the four different subprocesses: $q\bar{q}$, qg, qq, gg to the $O(\alpha_s{}^2)$ part of the DY cross section?
c. How does the cross section depend on the different choices made for the factorization scale μ^2 and the renormalization scale M^2?

TABLE I

The total cross section for Z-production (in nb) in three approximations at $Sp\bar{p}S$, Tevratron, LHC and SSC. The value between brackets is the sum of the contributions from $\Delta q\bar{q}$ and Δqg (both in $O(\alpha_s)$).

$\sqrt{S}$ [TeV]	0.63	1.8	16	40
Born	1.36	4.93	39.9	76.1
$O(\alpha_s)$	1.79 (−0.07)	6.16 (−0.52)	46.7 (−7.4)	86.2 (−17.0)
$O(\alpha_s^2)$	1.96	6.78	52.5	98.3

In Table I we have presented the total cross section for Z production for four different collider energies *i.e.* $\sqrt{S} = 0.63$ TeV, $\sqrt{S} = 1.8$ TeV, $\sqrt{S} = 16$ TeV and $\sqrt{S} = 40$ TeV. From this Table we infer that for increasing energies the K-factor gets smaller (see also Fig. 1). This is wholly due to the $O(\alpha_s)$ contribution. On the other hand the $O(\alpha_s{}^2)$ contribution slowly increases and becomes even larger than the $O(\alpha_s)$ one at SSC energies. This effect can be wholly attributed to the $O(\alpha_s)$ qg subprocess, which is always negative over the whole energy range. Since vector boson production at large energies is dominated by the small x_1, x_2 region in Eq. (1.3) this effect is not unexpected in view of the steep rise of the gluon distribution function at small x values. However one has to bear in mind that the extrapolation of the existing parametrizations of the gluon structure function to small x values cannot be trusted. Moreover we do not know the $O(\alpha_s{}^2)$ contribution of the qg subprocess to the K-factor yet. It is not impossible that the latter can compensate the effect of the $O(\alpha_s)$ part. Finally notice the size of the

K-factor at large hadron collider energies. It varies from 1.4 to 1.3 between $\sqrt{S} = 0.63$ TeV and $\sqrt{S} = 40$ TeV. This has to be compared with what happens at fixed target experiments ($\sqrt{S} = 20$ GeV) where K even can go up to about 2.4 [2]!

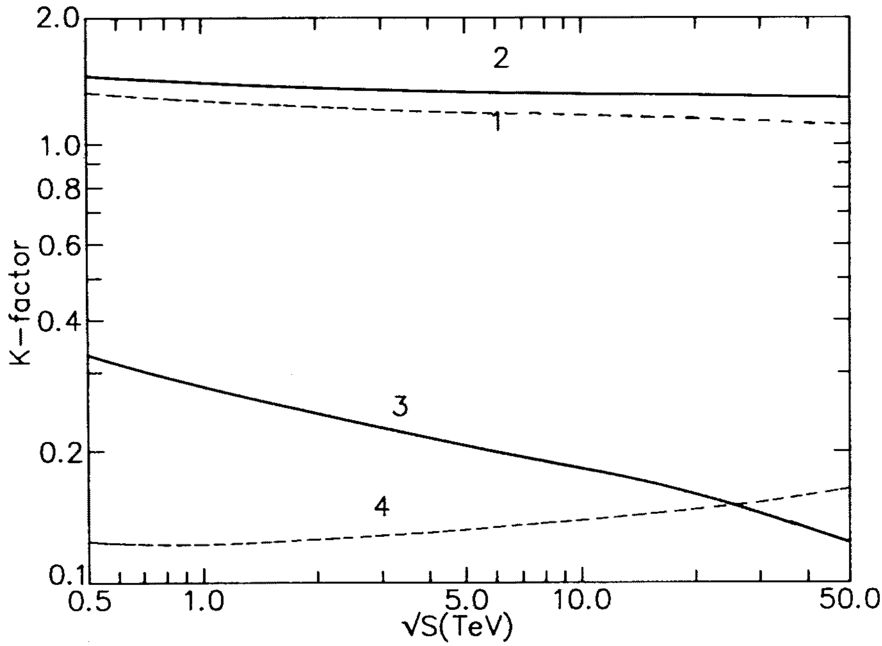

Fig. 1. The K-factor for Z-production at a p$\bar{\text{p}}$ collider. (1) K_1, (2) K_2, (3) $K^{(1)}$, (4) $K^{(2)}$.

In order to study the different contributions of the various subprocesses we introduce the following notations. The order α_s^icorrection to the theoretical K-factor is defined by

$$K^{(i)} = \frac{\sigma^{(i)}}{\sigma^{(0)}}. \tag{1.17}$$

Here $\sigma^{(0)}$ denotes the Born cross section and $\sigma^{(i)}$ is the $O(\alpha_s^i)$ contribution to the DY cross section. The $O(\alpha_s^2)$ corrected K-factor is given by

$$K_\ell = \sum_{i=0}^{\ell} K^{(i)}. \tag{1.18}$$

In Fig. 2 we have shown the contributions of the various subprocesses to the K-factor for Z-production. From this figure we infer that the q$\bar{\text{q}}$ subprocess (Eqs. (1.9) and (1.11)) dominates the K-factor followed by the qg

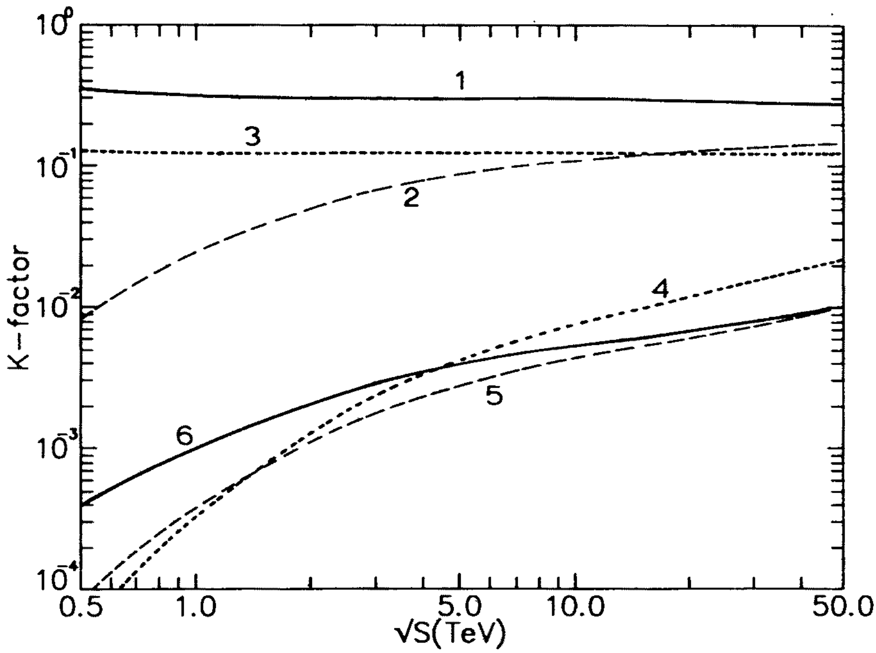

Fig. 2. The various contributions to the K-factor for Z-production at a p$\bar{\text{p}}$ collider. (1) $K^{(1)}_{\text{q}\bar{\text{q}}}$, (2) $-K^{(1)}_{\text{qg}}$, (3) $K^{(2)}_{\text{q}\bar{\text{q}}}$, (4) $K^{(2)}_{\text{gg}}$, (5) $K^{(2)}_{\text{qq}}$, (6) $K^{(2)}_{\text{q}\bar{\text{q}},\text{S}}$.

subprocess (Eq. (1.10)). The latter becomes only larger than the $O(\alpha_s^2)$ contributions to the q$\bar{\text{q}}$ process (Eq. (1.11)) in the case of SSC energies.

The dominance of the q$\bar{\text{q}}$ process can be attributed to the soft + virtual gluon terms appearing in Δq$\bar{\text{q}}$ provided the latter is calculated in the DIS scheme. On the other hand the gg subprocess never exceeds the 1% level. The same holds for q$\bar{\text{q}}|_\text{S}$ and the qq subprocess. At first sight it is unexpected that the gg subprocess is so small in view of the steep rise of the gluon distribution function at small x. In the case of heavy flavour production (see next Section) this property is one of the main reasons for the importance of this reaction. However the cross section is not only determined by the parton structure functions but also by the Wilson coefficient (correction term) as we will show below. Let us rewrite $W(\tau, Q^2)$ in the following form

$$W(\tau, Q^2) = \sum_{i,j} \int_\tau^1 \frac{dx}{x} \Phi_{ij}(x, \mu^2) \Delta_{ij}(\tau/x, Q^2, \mu^2, M^2) . \qquad (1.19)$$

where Φ_{ij} stands for the parton flux

$$\Phi_{ij}(x,\mu^2) = \int\limits_0^1 dx_1 \int\limits_0^1 dx_2\, \delta(x - x_1x_2) f_i^{\mathrm{H}_1}(x_1,\mu^2) f_j^{\mathrm{H}_2}(x_2,\mu^2)\,. \qquad (1.20)$$

The parton flux is characterized by the general property that is steeply rises as $x \to 0$ whereas it goes to zero when $x \to 1$. At very large S values we have $\tau = M_\mathrm{V}^2/S \ll 1$ which implies that $W(\tau,Q^2)$ is dominated by small x–region of the integrand in Eq. (1.19). Therefore the behaviour of $\Delta_{ij}(\tau/x)$ at $x = \tau$ is very important. The general behaviour of $\Delta_{ij}(x)$ near $x = 1$ for the various subprocesses is given by

$$\Delta \mathrm{q\bar{q}} \sim a_i \left(\frac{\ell n^i(1-x)}{1-x}\right)_+ + b_i\delta(1-x)\,, \qquad (1.21\mathrm{a})$$

$$\Delta \mathrm{qg} \sim a_i \ell n^i(1-x) + b_i\,, \qquad (1.21\mathrm{b})$$

$$\Delta \mathrm{qq} \sim (1-x)^a \quad (a > 0)\,, \qquad (1.21\mathrm{c})$$

$$\Delta \mathrm{gg} \sim (1-x)^b \quad (b > 0)\,, \qquad (1.21\mathrm{d})$$

$$\Delta \mathrm{q\bar{q}}, S \sim (1-x)^c \quad (c > 0)\,. \qquad (1.21\mathrm{e})$$

The vanishing of three last correction terms near $x = 1$ is caused by the two to three body phase space integrals which become zero at the boundary of phase space. This is the reason why these reactions gg, qq and $q\bar{\mathrm{q}}|_\mathrm{S}$ are suppressed with respect to the other ones.

TABLE II

$B \cdot \sigma_\mathrm{Z}$ (in pb) for $Sp\bar{p}S$ and Tevatron. We have used $B(\mathrm{Z} \to \mathrm{e^+e^-}) = 3.35 \times 10^{-2}$, $M_\mathrm{Z} = 91\,\mathrm{GeV}$, $\sin^2\theta_\mathrm{W} = 0.227$.

$\sqrt{s}$ [TeV]	0.63	1.8
Born	45.7	165
$O(\alpha_s)$	60.0	206
$O(\alpha_s^2)$	65.6	227
exp.	$70.4 \pm 5.5 \pm 4.0$ (UA2)	$197 \pm 12 + 32$ (CDF)

Finally we would like to investigate the scale dependence of $W(\tau,Q^2)$. In principle the latter should be scale independent since it is a physical quantity. However since the leading and the next to leading logs in $\Delta_{ij}(x,Q^2,\mu^2,M^2)$ are only calculated up to a finite order in α_s, $W(\tau,Q^2)$ will become scale dependent. There are many discussions in the literature concerning the choice of the right scale. Some groups prefer PMS [11]

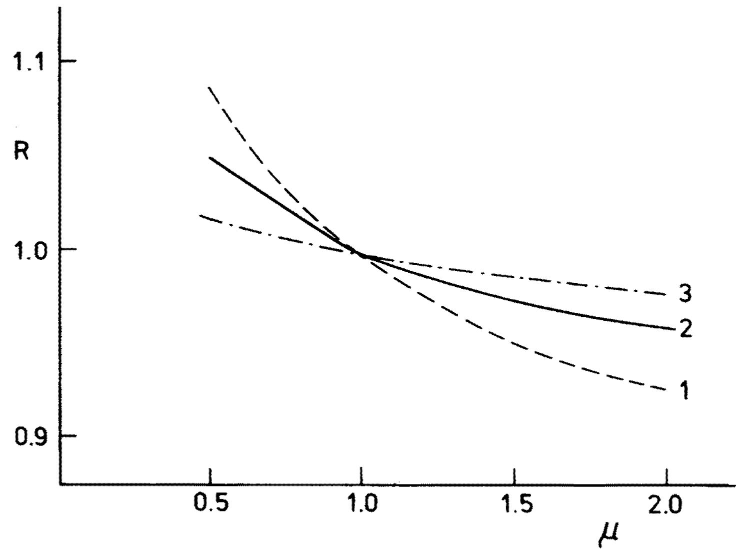

Fig. 3. Dependence of the mass factorization scale μ represented by the quantity $R = \sigma(\mu,\mu)/\sigma(M_V, M_V)$ for Z–production at $\sqrt{S} = 0.63$ TeV ($Sp\bar{p}S$). μ is expressed in units of M_V.

TABLE III

$B \cdot \sigma_{W^+ + W^-}$ (in pb) for $Sp\bar{p}S$ and Tevatron. We have used $B(W \to e\nu) = 0.109 : M_W = 80$ GeV, $\sin^2\theta_C = 0.05$.

$\sqrt{s}$ [TeV]	0.63	1.8
Born	479	1770
$O(\alpha_s)$	628	2210
$O(\alpha_s^2)$	690	2440
exp.	$660 \pm 15 \pm 37$	$2060 \pm 40 \pm 340$ (CDF)

whereas other people advocate FAC [12]. Other groups vary the scale between some canonical values [7]. The best solution to the problem is to show that the resulting expressions exhibit a very small variation under a wide range of scale choices. To my opinion semi leptonic processes like DY are a good candidate to satisfy this requirement since the lowest order contribution (Born) is independent of $\alpha_s(M)$. To simplify the discussion we choose in this lecture $\mu = M$. Independent variations of μ and M can be found in Ref. [5]. In Fig. 3 we have plotted the ratio $R = \sigma(\mu, M)/\sigma(M_V, M_V)|_{\mu=M}$ for Z production at $\sqrt{S} = 0.63$ TeV. We observe an improvement in the dependence of R on μ if higher order corrections are included. However at higher energies (see Ref. [5]) the $O(\alpha_s^2)$ corrected R is not better than the $O(\alpha_s)$ corrected one. On the contrary if we go to LHC or SSC energies the $O(\alpha_s^2)$ corrections lead to a larger deviation from 1 than the $O(\alpha_s^2)$ corrected R. This phenomenon has to be investigated. Probably this is due to the missing $O(\alpha_s^2)$ qg contribution or it can be attributed to the wrong scale dependence of the existing parton distribution functions at too small x–values. The same features as has been described above are also discovered for W–production (see Ref. [5]). Therefore there is no need to discuss this reaction. In Tables II and III we have compared our predictions for the processes $\mathrm{p}\bar{\mathrm{p}} \to Z \to \ell\bar{\ell}$ and $\mathrm{p}\bar{\mathrm{p}} \to W \to \ell\nu_\ell$ with the most recent results from the UA2 [3] and CDF [4] groups. From this table one concludes that the $O(\alpha_s)$ and $O(\alpha_s^2)$ predictions are in agreement with the data (UA2) whereas the Born approximation is not. This clearly indicates that QCD corrections are necessary to bring the DY cross section into agreement with experiment. However at this moment one cannot discriminate between the $O(\alpha_s)$ and $O(\alpha_s^2)$ corrected cross sections.

2. Heavy Flavour Production

During the last few years heavy flavour production called the attention of many experimentalists and phenomenologically oriented theoretical physicists. The reason for this interest can be summarized as follows [13]:

(a) The search of new quarks in particular the still evasive top quark.
(b) Bottom–anti-bottom production. Study of $\mathrm{b}\bar{\mathrm{b}}$ mixing, CP violation, determination of the Kobayashi–Maskawa matrix elements.
(c) Interpretation of single and double charged lepton signals.
(d) Background estimates in search of new physics.

On the Born level we have the following reactions [6,7]

$$O(\alpha_s^2) \qquad \mathrm{q} + \bar{\mathrm{q}} \to \mathrm{Q} + \bar{\mathrm{Q}}\,, \tag{2.1}$$

$$\mathrm{g} + \mathrm{g} \to \mathrm{Q} + \bar{\mathrm{Q}}\,, \tag{2.2}$$

where Q stands for the heavy quark (heavy flavour) and Q = c, b, t. In the next to leading order we encounter the processes

$$O(\alpha_s^3) \qquad \mathrm{q} + \bar{\mathrm{q}} \to \mathrm{Q} + \bar{\mathrm{Q}} \qquad \text{(1 loop)}, \tag{2.3a}$$

$$\mathrm{q} + \bar{\mathrm{q}} \to \mathrm{Q} + \mathrm{Q} + g\,, \tag{2.3b}$$

$$\mathrm{g} + \mathrm{g} \to \mathrm{Q} + \bar{\mathrm{Q}} \qquad \text{(1 loop)}, \tag{2.3c}$$

$$\mathrm{g} + \mathrm{g} \to \mathrm{Q} + \bar{\mathrm{Q}} + \mathrm{g}, \tag{2.3d}$$

$$\mathrm{g} + \mathrm{q}(\bar{\mathrm{q}}) \to \mathrm{Q} + \bar{\mathrm{Q}} + \mathrm{q}(\bar{\mathrm{q}})\,. \tag{2.3e}$$

The calculation of the single particle inclusive parton cross section is straightforward and for the details we refer to the literature [6,7]. Integrating over the whole phase space we obtain the total parton cross section

$$\hat{\sigma}_{ij}(s,m^2) = \frac{\alpha_s^2(\mu^2)}{m^2}\left\{f_{ij}^{(0)}(\eta) + 4\pi\alpha_s(\mu^2)\left[f_{ij}^{(1)} + \bar{f}_{ij}^{(1)}(\eta)\ln\frac{\mu^2}{m^2}\right]\right\},$$
$$\eta = \frac{s}{4m^2} - 1\,. \tag{2.4}$$

Here μ represents the factorization scale which has been put equal to the renormalization scale. The centre of mass energy squared of the incoming partons i and j is denoted by s and m stands for the heavy quark mass. The total cross section in Eq. (2.4) can only be expressed into scaling functions if the renormalization of the strong coupling constants α_s is chosen in such a way that the heavy flavours appearing in the internal loops are decoupled in the limit when the momenta entering the fermion loop contribution go to zero. Studying the shape of the various parton cross sections (see Refs [6,7]) we distinguish the following dominant production mechanisms.

2.1 Near threshold $s \sim 4m^2$

The Coulomb singularity originating from graphs where a massless vector boson (here the gluon) is exchanged between two heavy quark lines in the final state (Fig. 4a) leads to the following behaviour of the cross section

$$\hat{\sigma}_{ij}^{(1)}(s) \quad \sim \quad \frac{\pi^2}{s}, \quad s \to 4m^2\,. \tag{2.5}$$

Initial state gluon bremsstrahlung (ISGB) given by the momentum configuration of the out going gluon in Fig. 4b (with $\theta_g \to 0$ and $k_g \to 0$) yields the following behaviour.

$$\sigma_{ij}^{(1)} \quad \sim \quad \alpha_s \ln^2 8\eta \cdot \sigma_{ij}^{(0)}, \quad s \to \quad 4m^2\,. \tag{2.6}$$

Notice that ISGB gives a large enhancement to the cross section near threshold (Fig. 5).

2.2 Asymptotic region $s \gg m^2$

Here we have two dominant production mechanisms *i.e.* flavour excitation (FE) (Fig. 4c) and gluon splitting (GS) (Fig.4 d)¿ In this case the cross sections behave like

$$\sigma_{ij}^{(1)} \quad \sim \quad \frac{1}{m^2} \quad , \quad s \gg m^2\,. \tag{2.7}$$

This effect can be explained by the exchange of the massless vector boson (here gluon) in the t channel of the subprocesses $Q^* + g \to Q + g$ (EF) and

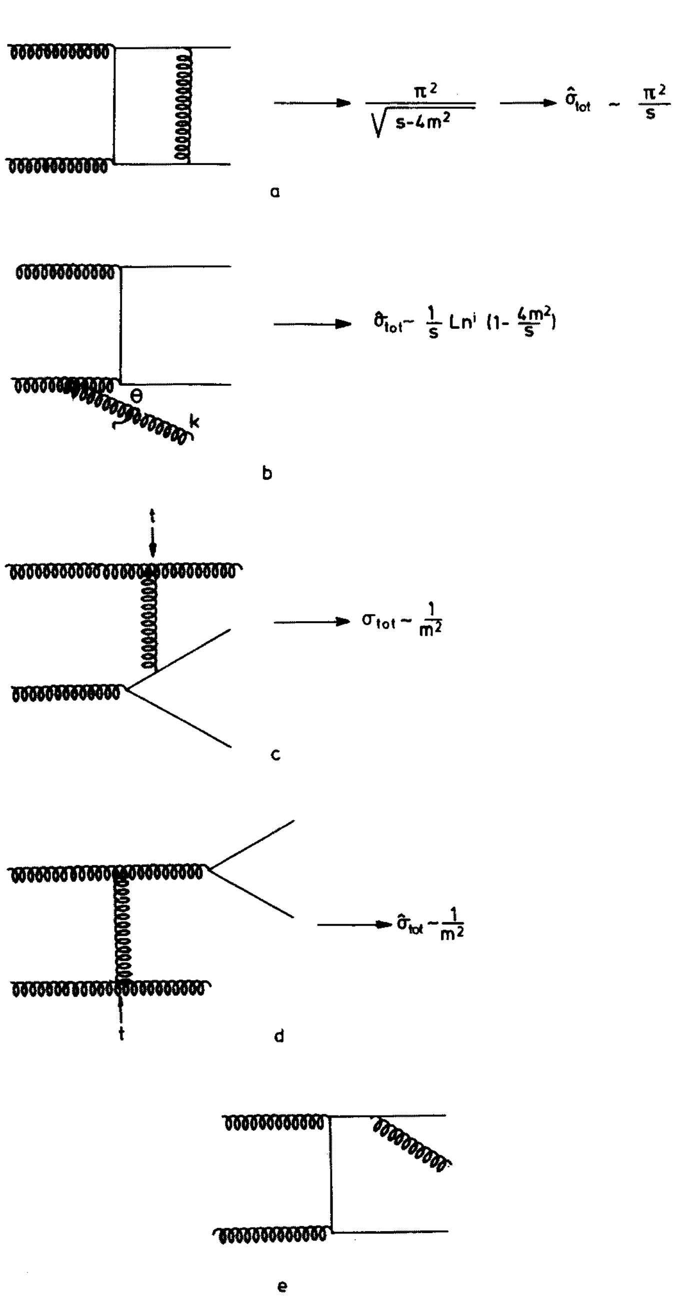

Fig. 4. Production mechanisms in heavy flavour production. (a) Coulomb singularity, (b) Initial state gluon bremsstrahlung (ISGB), (c) Flavour excitation (FE), (d) Gluon splitting (GS), (e) Final state quark fragmentation (FSQF).

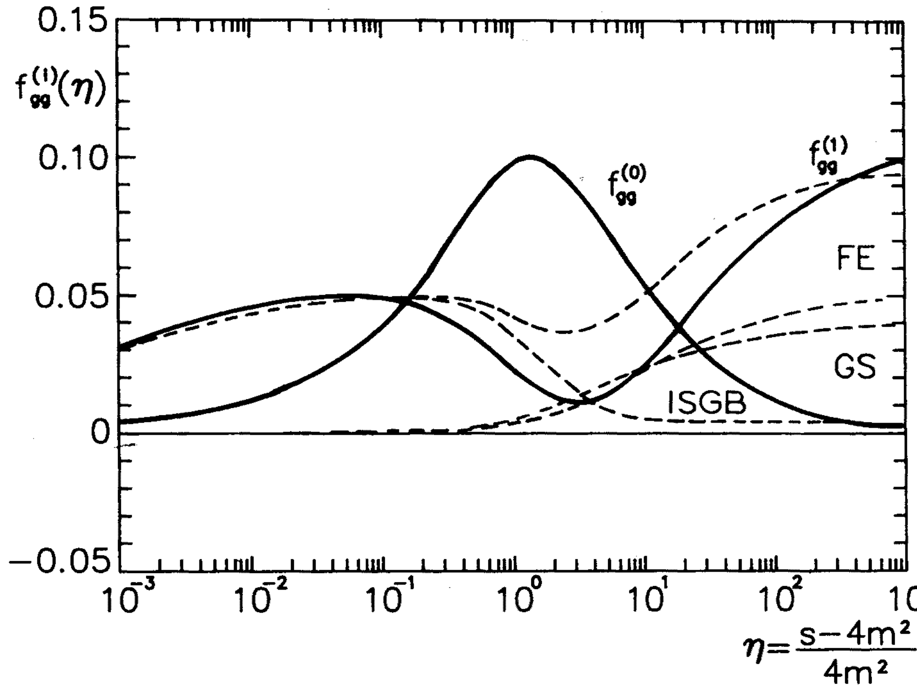

Fig. 5. The gluon–gluon contributions to the parton cross section plotted versus $\eta = s/4m^2 - 1$. The functions $f^{(0)}_{gg}, f^{(1)}_{gg}$ and $\bar{f}^{(1)}_{gg}$ are defined in Eq.(2.4). Solid (dashed) lines correspond to the exact (approximate) $O(\alpha_s^3)$ results. The contributions from initial state gluon bremsstrahlung (ISGB) flavour excitation (FE) and gluon splitting (GS) to the approximate $f^{(1)}_{gg}$ are shown separately.

$g + g \to g^* + g$ (GS) where the superscript * indicates that the particle is virtual. The main contribution to the total parton cross section at large s comes from the region $t \sim m^2$ (see Figs 4 c,d). Both mechanisms in the large plateau present in the total parton cross section at large s in the reactions gg (Figs 5,6) and gq($\bar{q}$).

2.3 Final state quark fragmentation (FSQF)

This process is indicated in Fig. 4e. Due to the KLN theorem [14] its contribution is negligible for the total cross section. Even in the case of the differential cross section where it gives rise to terms of the type $\ln s/m^2$ its contribution is unimportant in the whole s-region. Therefore we have not included this mechanism in the approximations outlined below.

The above "dominant" mechanisms inspired us to construct some approximations for the $O(\alpha_s)$ corrected parton cross section by using renormal-

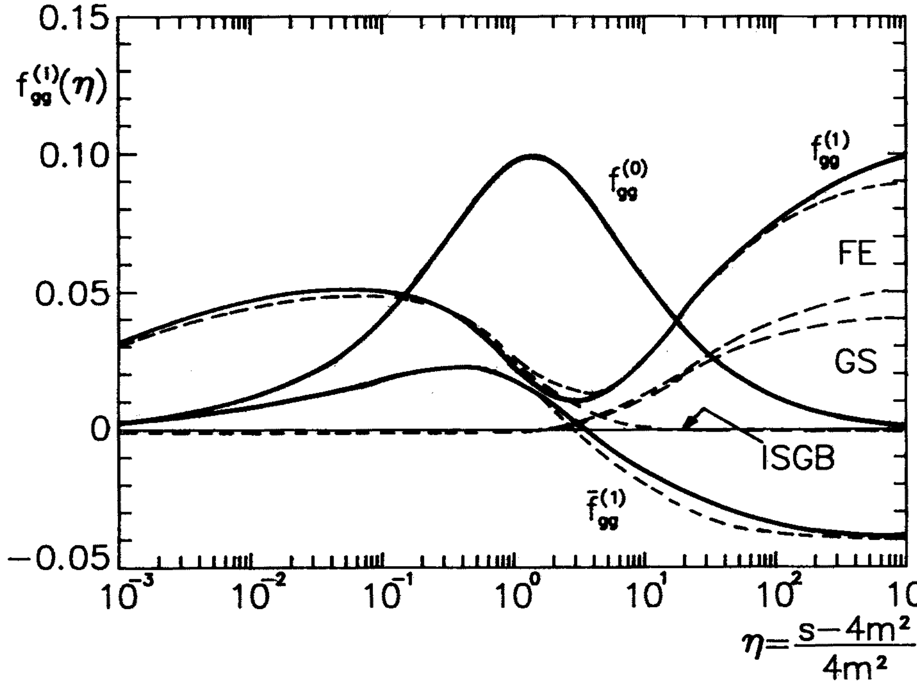

Fig. 6. Same as Fig. 5. The approximate contributions to $f(1)_{gg}$ are multiplied by the dumping (fudge) factors mentioned in Ref. [15]

ization group (mass factorization) methods (see Ref. [15]). Approximations based on physical principles are useful to understand the structure of the formulae obtained *via* an exact calculation. Moreover they lead to short expressions which can, provided the approximation is good enough, replace the very lengthy exact cross sections. In this way one gains much computer time.

In Fig. 5 we have plotted the exact as well as the approximate expressions for the function $f_{gg}^{(1)}$ ($\overline{\text{MS}}$ scheme). For small and large s we find good agreement. However the approximation expression is not able to describe the dip in the exact $f_{gg}^{(1)}$ which appears at moderate s values. Unfortunately that is just the region which gives an important contribution to the hadronic cross section when f_{ij} is convoluted with the gluon–gluon flux Φ_{gg} (see Eq. (1.20) and Table III). In order to improve the expressions we introduce a fudge factor [15]. The result of this operation is shown in Fig. 6 where the dip is now better reproduced by the new approximation. The effect on the total hadronic cross section for the process

$$p + \bar{p} \to Q + \bar{Q} + X \tag{2.8}$$

which is given by

$$\sigma(S,m^2) = \sum_{i,j} \int_{4m^2/S}^{1} dx\, \Phi_{ij}(x,\mu^2)\hat{\sigma}_{ij}(xS,m^2,\mu^2)\,, \tag{2.9}$$

has been shown in Tables I and II for top production at $\sqrt{S} = 0.63$ TeV and $\sqrt{S} = 1.8$ TeV respectively. The first striking result is that the main part of the $O(\alpha_s)$ correction can be attributed to the gg reaction. This is in contrast to what has been observed in the DY process. Further we see that the exact and the approximate corrections differ by about 25 to 30 %. The situation improves if the fudge factor is included except for the qg subprocess which is fortunately unimportant anyhow. The discrepancy between the exact and approximate hadron cross section is mainly due to the dip present in the gg and q$\bar{\text{q}}$ exact parton cross section. Unfortunately it is just the s region where the dip appears ($2 < s/4m^2 < 20$) which gives an important contribution to the integral in Eq.(2.9). As can be observed in Fig. 6 and Tables IV and V the introduction of the fudge factor improves the approximation for the total cross section. However this does not imply that also the differential distributions like $d^2\sigma/dydp_t$ (y = rapidity, p_t = transverse momentum of the heavy flavour) will become better.

TABLE IV

Total cross section in (pb) for top quark production $m_t = 40$ GeV) in p$\bar{\text{p}}$ collisions at $\sqrt{S} = 630$ GeV. The results of the exact $O(\alpha_s^3)$ calculations and the approximate formulae with and without the fudge factors are compared. The contributions from the gluon–gluon, quark–antiquark, and gluon–quark subprocesses are given separately. Also given are the respective Born contributions. The factorization scale $\mu = m_t$, and the DFLM structure function parametrization set 3 is used with $\Lambda_5 = 250$ MeV.

	gg	q$\bar{\text{q}}$	gq($\bar{\text{q}}$)	Sum
Born	164.6	332.9	0	497.5
exact $O(\alpha_s^3)$	147.1	61.9	−10.6	198.4
approx $O(\alpha_s^3)$	195.8	99.6	22.2	317.6
approx $O(\alpha_s^3)$ fudged	154.0	87.8	5.1	246.9

For that purpose we studied top production at $\sqrt{S} = 0.63$ TeV by looking at the three subprocesses gg, q$\bar{\text{q}}$ and gq($\bar{\text{q}}$) independently. For $y \geq 1.0$ or $p_t > 20$ GeV the curves of the exact and approximate differential cross section $d\sigma/dp_t$ come very close to each other. This is certainly the case for gg (Fig. 7) and q$\bar{q}$ (Fig. 8) but not for gq (Fig. 9). The latter is not unexpected since in Tables IV and V we already observed that the introduction of the fudge factor did not improve the approximation for the gq subprocess.

Finally we want to make some comments on the K-factor of heavy flavour production. Starting with the rapidity (y) distribution (see Fig. 10) for bottom production we observe that in the central region the lowest order cross section is much flatter than the $O(\alpha_s)$ corrected one. The p_t spectrum (see Fig. 11) shows no difference in shape between the Born and $O(\alpha_s)$ corrected cross section. The same holds for top production (Fig. 12). Notice the large K-factor, 2.5 for bottom and 1.4 top both at $\sqrt{S} = 1.8$ TeV, which is almost constant except near $p_t \sim 0$. This K-factor is larger than the one obtained for the DY process.

TABLE V

Same as Table I but for top production ($m_t = 120$ GeV) at Fermilab collider c.m. energy $\sqrt{S} = 1.8$ TeV. The DFLM structure function parametrization set 2 with $\Lambda_5 = 173$ MeV is used.

	gg	q$\bar{q}$	gq($\bar{q}$)	Sum
Born	6.50	19.33	0	25.83
exact $O(\alpha_s^3)$	4.96	2.98	−0.45	7.49
approx $O(\alpha_s^3)$	6.40	4.66	0.79	11.85
approx $O(\alpha_s^3)$ fudged	5.16	4.12	0.19	9.47

Before finishing this lecture I would like to make some additional comments.

(a) For p$\bar{p}$ colliders the gg subprocess is the dominant production mechanism in particular for c- and b-production. In the case of top production the Born contribution from the q$\bar{q}$ subprocess becomes important too.

(b) The subprocess q$\bar{q}$ and gq($\bar{q}$) cause an asymmetry in the rapidity (y) distribution between the heavy quark and anti-quark [6,7]. Maybe this will be observable at fixed target experiments.

(c) The contribution due to the gq($\bar{q}$) subprocess is small in all regions of phase space.

(d) The figures show large radiative corrections at the centre of the rapidity plot. The shape of the p_t spectrum is unaffected by the $O(\alpha_s)$ corrections. There is a large K-factor which is very sensitive to changes in the mass factorization and renormalization scales [7]. This is not surprising since the Born cross section is already of $O(\alpha_s^2)$. Therefore perturbative

QCD gives a much less reliable prediction for heavy flavour production than it does for the DY process.

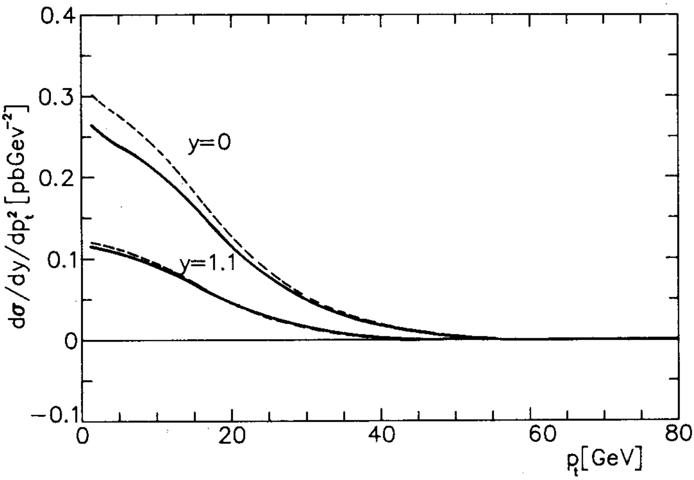

Fig. 7. The contributions from the gluon–gluon subprocess to the differential cross section for p+$\bar{\text{p}}$ $\rightarrow$ Q+$\bar{\text{Q}}$+X at two different rapidity values $y = 0$ and $y = 1.1$. Our exact results are shown for $\sqrt{S} = 630$ GeV with $m_Q = 40$ GeV/c^2 and $\Lambda_5 = 173$ MeV. The factorization scale $\mu = \sqrt{m_Q^2 + p_t^2}$. We also show the results of our approximate calculations.

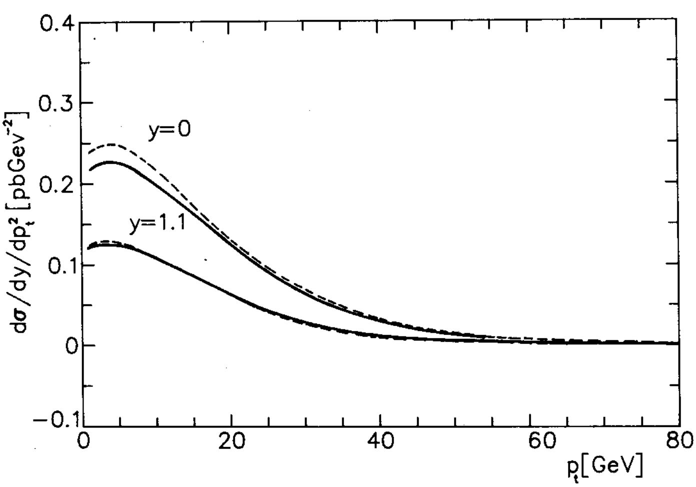

Fig. 8. The same as in Fig. 7 but the quark–antiquark subprocess.

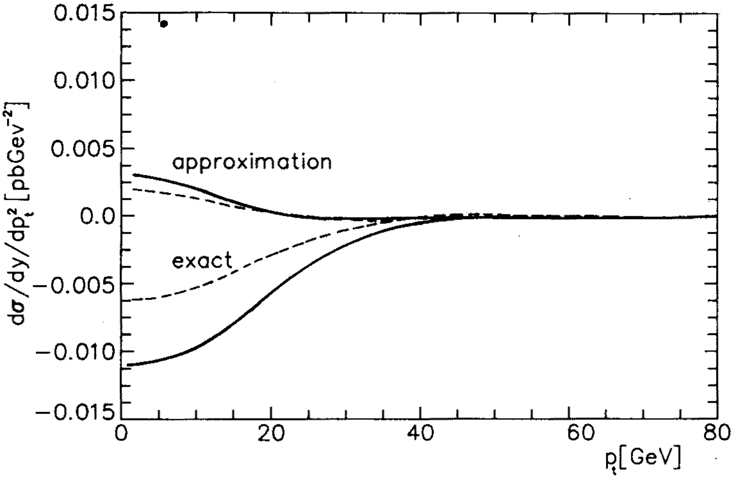

Fig. 9. The same as in Fig. 7, but for the gluon–(anti)quark subprocess. Here the lower curves refer to our exact calculations and the upper ones to our approximations.

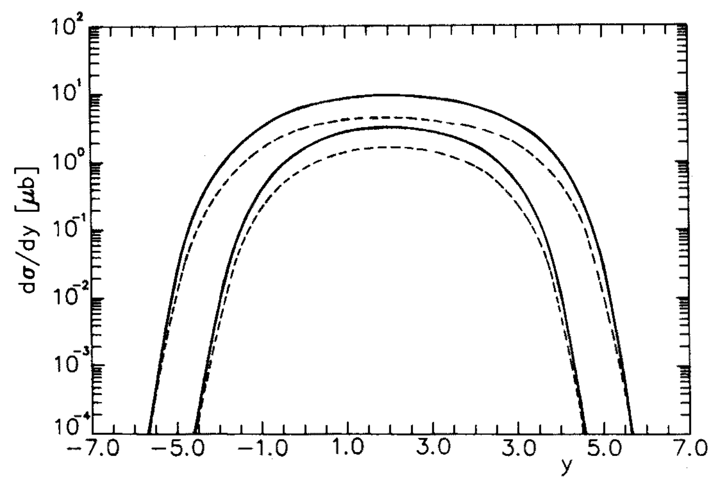

Fig. 10. The rapidity distribution for $p + \bar{p} \to b + X$ with $m_b = 4.75 \mathrm{GeV}/c^2$, $\mu = \sqrt{m_b^2 + p_t^2}$ at $\sqrt{S} = 630$ GeV and $\sqrt{S} = 1.8$ TeV. The upper curves refer to the higher energy.

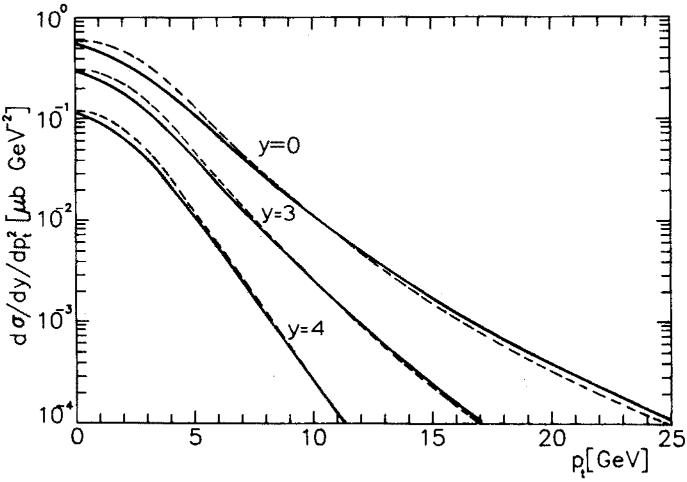

Fig. 11. The differential cross section for $p + \bar{p} \rightarrow b + X$ with $m_b = 4.75$ GeV/c^2 and $\mu = \sqrt{m_b^2 + p_t^2}$ at $\sqrt{S} = 1.8$ TeV. The cross section is shown at different values of rapidity for (1) dashed lines: lowest order contribution scaled by an arbitrary factor (here 2.5); (2) solid lines: full order α_s^3 calculation.

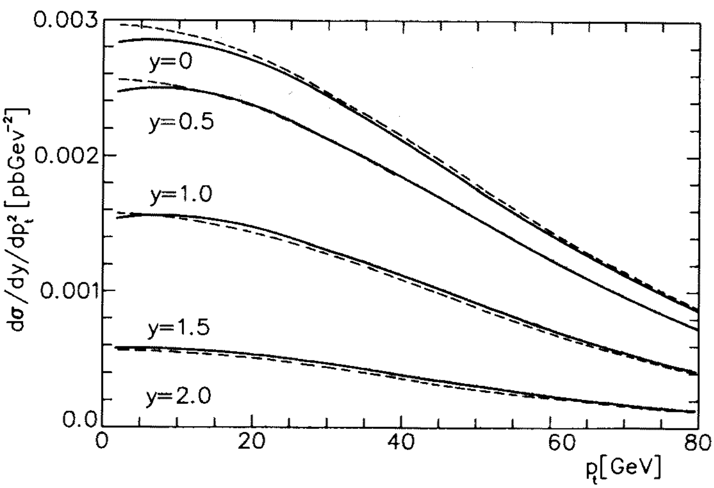

Fig. 12. The differential cross section $p+\bar{p} \rightarrow t+X$ with $m_t = 120$GeV/c^2 and $\mu = \sqrt{m_t^2 + p_t^2}$ at $\sqrt{S} = 1.8$ TeV. The cross section is shown at different values of rapidity for (1) dashed lines: lowest order contributions scaled by an arbitrary factor (here 1.4); (2) solid lines: full order α_s^3 calculation.

REFERENCES

[1] Proceedings of the XXIV International Conference on High Energy Physics. Munich, Fed. Rep. of Germany, August 4–10, 1988, eds. R. Kotthaus, J. H. Kühn, see the contributions by R. K. Ellis, p. 48, and W. J. Stirling,p. 733.

[2] J. Badier et al., *Phys. Lett.* **B89**, 145 (1979); E. Anassontzis et al.,*Phys. Rev.* **D38**, 1397 (1988); J. S. Conway et al., *Phys. Rev.* **D39**,92 (1989); K. Freudenreich, Lepton pair production in hadron–hadron collisions, habilitation thesis, Dec. 1988, ETH Zürich.

[3] UA2 collaboration: J. Alitti et al., CERN–EP/90–20.

[4] CDF collaboration: *Production properties of the W, Z bosons*, P. F. Derwent, 25th Rencontres de Moriond, Les Arcs, Savoie — France, March 1990.

[5] T. Matsuura, S.C. van der Marck, W. L. van Neerven, *Phys. Lett.* **B211**, 191 (1988), *Nucl. Phys.* **B319**, 570 (1989); T. Matsuura, R. Hamberg, W. L. van Neerven, DESY 90-031, to be published in *Nucl. Phys.* **B**.

[6] W. Beenakker, H. Kuijf, W. L. van Neerven, J. Smith, *Phys. Rev.***D40**,54 (1989); W. Beenakker, W. L. van Neerven, R. Meng, G. A. Schuler, J. Smith, DESY 90-064.

[7] P. Nason, S. Dawson, R.K. Ellis, *Nucl. Phys.* **B303**, 607 (1988); **B327**, 54 (1989).

[8] G. Altarelli, *Phys. Rep.* **81**, 1 (1982).

[9] M. Diemoz, F. Ferroni, E. Longo, G. Martinelli, *Z. Phys.* **C39**, 21 (1988).

[10] G. Altarelli, M. Diemoz, G. Martinelli, P. Nason, *Nucl. Phys.* **B308**, 724 (1988).

[11] P. M. Stevenson, *Phys. Rev.***D23**,2916 (1981);*Nucl. Phys.* **B203**, 472 (1982)

[12] G. Grunberg, *Phys. Lett.* **95B**, 70 (1980).

[13] A. Ali, B. van Eijk, I. ten Have, *Nucl. Phys.* **B291**, 1 (1987); UA1 collaboration, C. J. Albajar et al., *Z. Phys.* **C37**, 489 (1988); *Phys. Lett.* **B186**, 237 (1987).

[14] T. Kinoshita, *J. Math. Phys.* **3**, 650 (1962); T. D. Lee, M. Nauenberg, *Phys. Rev.***B133**, 1549 (1964).

[15] R. Meng, G. A. Schuler, J. Smith, W. L. van Neerven, *Nucl. Phys.* **B339**, 325 (1990).